SIAM J. APPL. MATH.
Vol. 67, No. 6, pp. 1654–1674

ATTRACTORS IN CONFINED SOURCE PROBLEMS FOR COUPLED NONLINEAR DIFFUSION*

D. V. STRUNIN†

Abstract. In processes driven by nonlinear diffusion, a signal from a concentrated source is confined in a finite region. Such solutions can be sought in the form of power series in a spatial coordinate. We use this approach in problems involving coupled agents. To test the method, we consider a single equation with (a) linear and (b) quadratic diffusivity in order to recover the known results. The original set of PDEs is converted into a dynamical system with respect to the time-dependent series coefficients. As an application we consider an expansion of a free turbulent jet. Some example trajectories from the respective dynamical system are presented. The structure of the system hints at the existence of an attracting center manifold. The attractor is explicitly found for a reduced version of the system.

Key words. nonlinear diffusion, attractor, turbulence

AMS subject classifications. 35K55, 76F20, 76F60

DOI. 10.1137/060657923

1. Introduction.

A variety of physical processes are described by the nonlinear diffusion equations

$$\partial_t K = (-1)^n \nabla \left(K^m \nabla \, \Delta^n K \right), \tag{1}$$

where $n \geq 0$ is an integer and $m > 0$. In the particular case of $n = 0$, (1) becomes the second-order diffusion equation

$$\partial_t K = \nabla \left(K^m \nabla K \right). \tag{2}$$

An important common property of the nonlinear diffusion (2) and its higher-order generalizations (1) is the finiteness of the speed of a signal propagation. If the signal is initially confined in a finite region so that it is identically equal to zero beyond the region, the signal remains confined during the dynamics. This property distinguishes the nonlinear diffusion from the linear diffusion ($m = 0$), where the signal instantaneously propagates to infinity.

The range of processes described by (1)–(2) is wide. The second-order equations (2) are known as the porous medium equations and appear in models of gas filtration in porous media [1, 2] and thin fluid films in a gravitational field ($m = 3$) [3]. The fourth-order equations ($n = 1$) emerge in lubrication models for thin viscous films ($m = 3$) and Hele–Shaw flows ($m = 1$). The sixth-order models ($n = 2$) are relevant to the process of isolation oxidation of silicon ($m = 3$) [4]. The models with $m = 3$ and different values of n describe thin viscous droplets driven by different factors: gravity ($n = 0$), surface tension ($n = 1$), and an elastic plate ($n = 2$).

Various mathematical aspects of the second-order equation (2) are analyzed in [5, 6, 7]; the fourth-order model is investigated, for example, in [8]. Numerical schemes for

*Received by the editors April 22, 2006; accepted for publication (in revised form) April 24, 2007; published electronically September 26, 2007.
http://www.siam.org/journals/siap/67-6/65792.html

†Department of Mathematics and Computing, University of Southern Queensland, Toowoomba, QLD 4350, Australia (strunin@usq.edu.au).

solving the fourth- and sixth-order equations using finite differences or finite elements are developed in [9, 10, 11].

In this paper we focus on attractors in coupled nonlinear diffusion with confined sources when there are more than one diffusing agent.

To give an example of an attractor in nonlinear diffusion we consider the second-order equation (2) in one dimension, $\partial_t K = \partial_x(K^m \partial_x K)$. Its solution evolving from a confined initial profile is attracted to the universal regime [12, 13],

$$K(x,t) = \frac{\gamma(m)}{t^{1/(m+2)}} \left(\xi_0^2 - \xi^2\right)^{1/m}, \tag{3}$$

where

$$\xi = \frac{x}{t^{1/(m+2)}}, \quad \xi_0 = \left[\frac{\Gamma\left(\frac{1}{m}+\frac{3}{2}\right)}{\gamma(m)\sqrt{\pi}\,\Gamma\left(\frac{1}{m}+1\right)} E\right]^{\frac{m}{m+2}}, \quad \gamma(m) = \left[\frac{m}{2(m+2)}\right]^{\frac{1}{m}},$$

Γ is the gamma-function, and E is the integral

$$E = \int_{-\infty}^{\infty} K(x,t)\,dx,$$

which conserves during the evolution. For our purposes it is convenient to write the attractor (3) in the form

$$K(x,t) = \frac{\alpha}{t^{1/(m+2)}} \left(1 - \frac{\beta}{t^{2/(m+2)}}\, x^2\right)^{1/m}, \tag{4}$$

where α and β are the coefficients depending on m and E.

Similar attractors exist for the higher-order equations (1). For example, in one dimension for $m = 1$ and $n = 1$, i.e., for the fourth-order equation $\partial_t K = \partial_x(K\partial_x^3 K)$, the attractor is [14]

$$K(x,t) = \frac{1}{120\, t^{1/5}} \left(\xi_0^2 - \xi^2\right)^2,$$

where

$$\xi = \frac{x}{t^{1/5}}, \quad \xi_0 = \left(\frac{225E}{2}\right)^{1/5}.$$

Recently in [11], (1) was analyzed numerically for $n = 2$ and $m = 1$, that is, the sixth-order equation $\partial_t K = \partial_x(K\partial_x^5 K)$. It was proved that the solution converges to the attractor found in [14].

Many processes involve more than one diffusing agent. For example, in a free turbulent jet the diffusing turbulent energy is coupled with the diffusing momentum. We analyze this process later in the paper. In the multicomponent problems an important question to answer is whether there exists an attractor.

Another motivation for us to analyze this particular phenomenon stems from fluid mechanics, where an expansion of a jet from a narrow pulse is a natural problem formulation. For other processes, other regimes can be of interest. For example, in the isolation oxidation of silicon, traveling waves are of major interest [10].

In this paper we take an approach in which confined solutions are sought as power-series in a spatial coordinate. The diffusion of the turbulent jet is one of many problems to which this approach is applicable.

Previously [15] we studied the expansion of the turbulent jet using a *nonlocal* version of the K-ℓ model of turbulence (see, e.g., the review [16]).

In the present paper we use the K-ε model [17, 18], which is *local*. The locality enables us to convert the governing PDEs into a set of ODEs. Thus, the problem transforms into a standard dynamical system formulation, in which framework we look for an attractor.

As a first step, in section 2 we test our approach on some standard problems to recover known results. Then, in section 3 the approach is applied to the turbulent jet. In section 4 we analyze in detail its reduced version. The conclusions are given in section 5.

2. Power-series approach. In this section we formulate our approach and test it on simple problems. We consider the nonlinear diffusion with linear and then quadratic diffusivity.

2.1. Diffusion with linear diffusivity. Consider (2) with $m = 1$:

$$\partial_t K = \partial_x (K \partial_x K). \tag{5}$$

The long-term asymptotics (4) of its pulse solution is

$$K = \frac{\alpha}{t^{1/3}} \left(1 - \beta \frac{x^2}{t^{2/3}} \right) \tag{6}$$

or

$$K = a(t) \left[1 - b(t) x^2 \right] \tag{7}$$

with

$$a(t) = \frac{\alpha}{t^{1/3}}, \quad b(t) = \frac{\beta}{t^{2/3}}.$$

For finite times, assuming an initial pulse is symmetric, we seek a solution in the form

$$K(x,t) = A(t) \left[1 - B_2(t) x^2 - B_4(t) x^4 - B_6(t) x^6 - \cdots \right], \tag{8}$$

where $A(t) > 0$ is the value of K at $x = 0$. Expression (8) is acceptable as long as it gives a positive answer. Thus, (8) represents the solution on some interval $0 \le x \le h(t)$, where $h(t)$ is the position of the front in which $K[h(t), t] = 0$. Beyond the front, for $x > h(t)$, formula (8) does not apply; we assume $K(x,t) \equiv 0$ instead. With various initial values $B_k(0)$, $k = 2, 4, \ldots$, the form (8) expresses a wide class of symmetric initial conditions. Apparently $B_k(t)$ are proportional to the Taylor-series coefficients of $K(x,t)$.

Substituting (8) into (5), collecting the terms with the same powers of x, and equating the coefficients gives

$$\begin{aligned} \dot{A} &= -2A^2 B_2, \\ \dot{B}_2 &= -4AB_2^2 + 12AB_4, \\ \dot{B}_4 &= -28AB_2B_4 + 30AB_6, \\ \dot{B}_6 &= -54AB_2B_6 - 28AB_4^2 + 56AB_8, \\ &\ldots. \end{aligned} \tag{9}$$

The system (9) contains no linear terms; however, we can "create" those by modifying time. Divide all the equations in (9) by AB_2 and introduce the new time τ by

$$\frac{d}{AB_2\,dt} = \frac{d}{d\tau} \equiv ()'. \tag{10}$$

Then system (9) transforms into

$$\begin{aligned} A' &= -2A, \\ B_2' &= -4B_2 + 12\frac{B_4}{B_2}, \\ B_4' &= -28B_4 + 30\frac{B_6}{B_2}, \\ B_6' &= -54B_6 - 28\frac{B_4^2}{B_2} + 56\frac{B_8}{B_2}, \\ &\dots. \end{aligned} \tag{11}$$

Looking at the coefficients of the linear terms we notice a considerable spectral gap between the coefficient -4 at B_2 in the equation $B_2' = \dots$ and the coefficient -28 at B_4 in the equation $B_4' = \dots$. Therefore we can expect that B_4 and the subsequent B_k, $k = 6, 8, \dots$, will decay much faster than A and B_2. This is confirmed numerically as demonstrated by Figure 1. The plot shows a family of trajectories for the truncated system formed by the dynamic equations for B_2, B_4, and B_6 in (11) with the term containing B_8 removed. The figure gives three different views of the same trajectories to expose the faster decay of B_4 and B_6 in comparison to B_2.

The numerical results in this paper are obtained with the MATLAB solver DAE2 developed by Roberts [19].

It is interesting to evaluate the contribution of different terms, $(-B_k x^k)$, in the function

$$1 - B_2x^2 - B_4x^4 - B_6x^6 - \cdots \tag{12}$$

defining the shape of $K(x,t)$. Let us compare the terms for the largest value of x inside the signal, that is, the coordinate of the front, $x = h(t)$. Retain the first three terms in (12), presuming that the input of the sixth- and higher-order terms is negligible. On the front the signal vanishes, and therefore approximately

$$1 - B_2h^2 - B_4h^4 = 0.$$

From here

$$h^2 = \left(-B_2 + \sqrt{B_2^2 + 4B_4}\right) \Big/ (2B_4). \tag{13}$$

Further, if we suppose that

$$B_4 \ll B_2/h^2, \tag{14}$$

then the fourth-order term appears to be negligible compared to the quadratic term. Inserting (13) into (14) and rearranging, we obtain

$$B_4 \ll 2B_2^2. \tag{15}$$

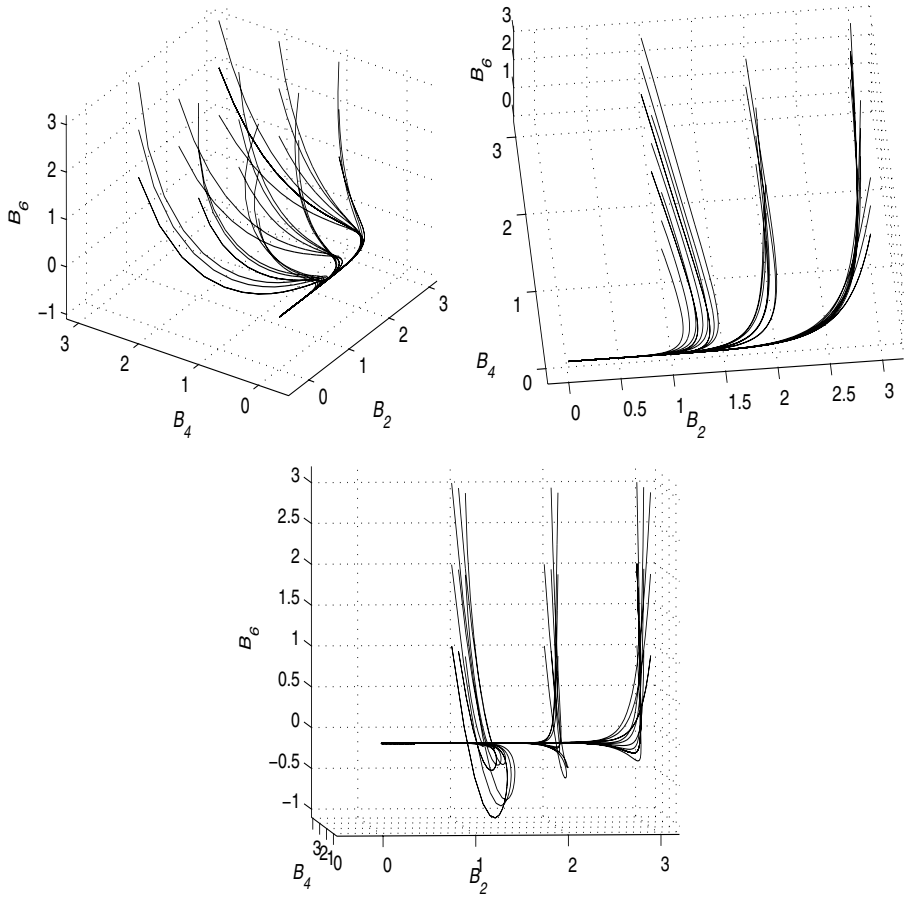

FIG. 1. *Solutions of truncated system* (11).

In the numerical experiments the condition (15) was satisfied several orders over. Tracking the value of $h(t)$ directly from the numerical experiment confirms the negligible contribution of the fourth- and higher-order terms.

Thus, the power-series approach recovered the expected result that (6) is indeed the attractor for the diffusion problem with the linear diffusivity.

2.2. Diffusion with quadratic diffusivity. In this section we consider the diffusion equation with quadratic diffusivity,

$$\partial_t K = \partial_x \left(K^2 \partial_x K \right). \tag{16}$$

Its pulse solution (4) has the form

$$K = \frac{\alpha}{t^{1/4}} \left(1 - \beta \frac{x^2}{t^{1/2}} \right)^{1/2}. \tag{17}$$

Expanding (17) into the Taylor-series, we get

$$K(x,t) = a(t) \left[1 - b_2(t) x^2 - b_4(t) x^4 - b_6(t) x^6 - \cdots \right], \tag{18}$$

where

$$
\begin{aligned}
&b_2(t) = \beta\frac{1}{2\sqrt{t}}, \quad b_4(t) = \beta^2\frac{1}{8t},\\
&b_6(t) = \beta^3\frac{1}{16t^{3/2}}, \quad b_8(t) = \beta^4\frac{5}{128t^2},\\
&\ldots.
\end{aligned}
\tag{19}
$$

It converges for $\beta x^2/t^{1/2} \le 1$, that is, for all x of interest, $0 \le x \le h(t) = t^{1/2}/\beta$. Any b_k in (19) can be expressed through a selected one, for instance, b_2:

$$
b_4 = \frac{1}{2}b_2^2, \quad b_6 = \frac{1}{2}b_2^3, \quad b_8 = \frac{5}{8}b_2^4, \quad \ldots. \tag{20}
$$

Expressions (20) describe the attractor which we intend to reproduce by our approach. As in the previous section, we seek a power-series solution of (16),

$$
K(x,t) = A(t)\,[1 - B_2(t)x^2 - B_4(t)x^4 - B_6(t)x^6 - \cdots]. \tag{21}
$$

Substituting (21) into (16) leads to

$$
\begin{aligned}
&\dot{A} = -2A^3B_2,\\
&\dot{B}_2 = -10A^2B_2^2 + 12A^2B_4,\\
&\dot{B}_4 = -58A^2B_2B_4 + 30A^2B_6 + 10A^2B_2^3,\\
&\dot{B}_6 = -110A^2B_2B_6 + 56A^2B_2^2B_4 - 56A^2B_4^2 + 56A^2B_8,\\
&\dot{B}_8 = -178A^2B_2B_8 + 90A^2B_2^2B_6 + 90A^2B_2B_4^2 - 180A^2B_4B_6 + 90A^2B_{10},\\
&\ldots.
\end{aligned}
\tag{22}
$$

We divide all the equations in (22) by A^2B_2 and introduce the new time τ by

$$
\frac{d}{A^2B_2\,dt} = \frac{d}{d\tau} \equiv ()'. \tag{23}
$$

As a result, system (22) transforms into the following form with linear terms:

$$
\begin{aligned}
&A' = -2A,\\
&B_2' = -10B_2 + \frac{12B_4}{B_2},\\
&B_4' = -58B_4 + \frac{30B_6}{B_2} + 10B_2^2,\\
&B_6' = -110B_6 + 56B_2B_4 - \frac{56B_4^2}{B_2} + \frac{56B_8}{B_2},\\
&B_8' = -178B_8 + 90B_2B_6 + 90B_4^2 - \frac{180B_4B_6}{B_2} + \frac{90B_{10}}{B_2},\\
&\ldots.
\end{aligned}
\tag{24}
$$

Consider only three dynamic equations for B_2, B_2, and B_4 with the term containing B_8 omitted. A set of trajectories for such a system is shown in Figure 2. It is clearly seen from different angles that the trajectories are attracted to a single curve or a one-dimensional manifold. It can be shown that the curve is described by

$$
B_4 = \gamma B_2^3, \quad B_6 = \mu B_2^3, \tag{25}
$$

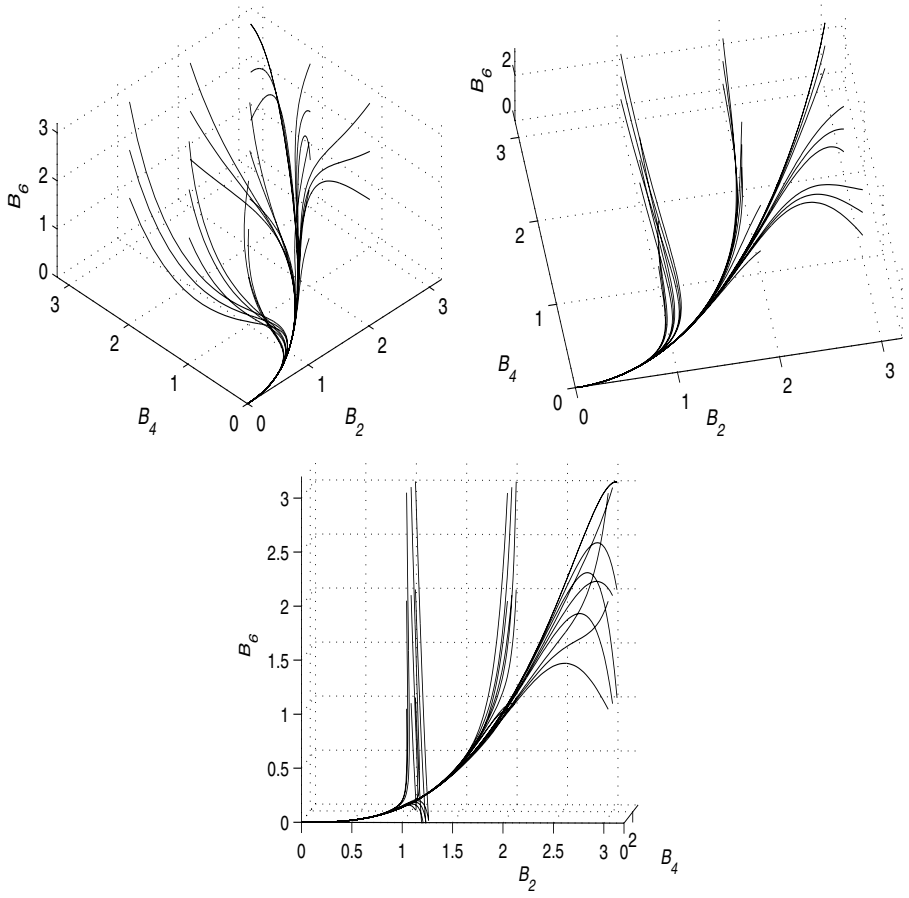

FIG. 2. *Solutions of truncated system* (24).

where γ and μ are parameters. It is interesting to compare them to their values on the attractor defined by (20). We substitute (25) into (24) to obtain

$$
\begin{aligned}
B_2' &= (-10 + 12\gamma)\, B_2, \\
B_2' &= \left(-29 + \frac{15\mu}{\gamma} + \frac{5}{\gamma}\right) B_2, \\
B_2' &= \left(-\frac{110}{3} + \frac{56\gamma}{3\mu} - \frac{56\gamma^2}{3\mu}\right) B_2.
\end{aligned}
\tag{26}
$$

As each of the equations in (26) describes the motion on the attractor, they all must coincide. So must the coefficients at B_2 in their right-hand sides. This leads to two algebraic equations with respect to γ and μ, giving approximately $\gamma = 0.31$, $\mu = 0.14$. Compare these to the exact values from (20),

$$\gamma_* = 1/2 = 0.5, \quad \mu_* = 1/2 = 0.5.$$

The departure from the exact values can be diminished by involving more equations. For the four-equation system with respect to B_2, B_4, B_6, and B_8, with the term

containing B_{10} excluded, we have

$$B_4 = \gamma B_2^3, \quad B_6 = \mu B_2^3, \quad B_8 = \lambda B_2^4. \tag{27}$$

Inserting (27) into (24) leads to a system of three equations, with respect to γ, μ, and λ, having the approximate solution $\gamma = 0.35$, $\mu = 0.20$, $\lambda = 0.11$. Note that from (20) the exact value for λ is $\lambda_* = 5/8 = 0.62$. To improve the approximation further, more equations have to be involved.

In summary, we reproduced the well-known fact that for the diffusion with quadratic diffusivity the trajectories converge to a one-dimensional manifold representing the similarity regime (17).

3. The K-ε model of a turbulent jet. Consider a turbulent jet created in an unbounded motionless fluid by a quick impulse shaped in space as a narrow flat layer. For instance, some amount of fluid is quickly injected. The velocity shear between the jet and surrounding fluid pumps up the kinetic energy of turbulence. The turbulent region expands and, in the long term, the energy decays due to the geometric effect of expansion and the loss into heat caused by intersections of vortices (we will call this loss simply dissipation).

The expansion is driven by the turbulent diffusion which is essentially nonlinear. As a consequence, the jet has a sharp front similar to the above examples. However, the dynamics is complicated by the coupling between the kinetic energy, dissipation, and momentum. The K-ε model of turbulence [17, 18] is written

$$\begin{aligned}
\partial_t K &= \alpha_1 \partial_x \left(\frac{K^2}{\varepsilon} \partial_x K \right) + \alpha_2 \frac{K^2}{\varepsilon} \left(\partial_x u \right)^2 - \alpha_3 \varepsilon, \\
\partial_t \varepsilon &= \beta_1 \partial_x \left(\frac{K^2}{\varepsilon} \partial_x \varepsilon \right) + \beta_2 K \left(\partial_x u \right)^2 - \beta_3 \frac{\varepsilon^2}{K}, \\
\partial_t u &= \chi \partial_x \left(\frac{K^2}{\varepsilon} \partial_x u \right).
\end{aligned} \tag{28}$$

In (28) the coordinate x is directed across the flat turbulent layer originating in its middle, K stands for the kinetic energy of turbulent pulsations per mass unit, and ε is the dissipation of the turbulent energy; $\alpha_{1,2,3}$, $\beta_{1,2,3}$, and χ are nondimensional coefficients. The system (28) is nondimensional, obtained from dimensional form by using some useful scales, for example, the average initial velocity across the jet, U, as the velocity scale; the initial width of the jet, $2h$, as the length scale; U^2 as the turbulent energy scale; U^3/h as the dissipation rate scale; and h/U as the time scale.

The initial profiles of K, ε, and u across the turbulent layer are assumed to have dome-like forms. We assume that they are symmetric with respect to the middle of the layer. On the edge, or front, of the jet the functions descend to zero and remain zero beyond the front (see the discussion further in this section).

We look for the power-series solutions of (28),

$$\begin{aligned}
K &= A(t) \left[1 - B_2(t) x^2 - B_4(t) x^4 - B_6(t) x^6 - \cdots \right], \\
\varepsilon &= P(t) \left[1 - R_2(t) x^2 - R_4(t) x^4 - R_6(t) x^6 - \cdots \right], \\
u &= M(t) \left[1 - N_2(t) x^2 - N_4(t) x^4 - N_6(t) x^6 - \cdots \right].
\end{aligned} \tag{29}$$

Substituting the series (29) into the dynamic equations (28) leads to

$$
\begin{aligned}
\dot{A} &= -\alpha_1 \frac{2A^3 B_2}{P} - \alpha_3 P,\\
\dot{P} &= -\beta_1 2A^2 R_2 - \beta_3 \frac{P^2}{A},\\
\dot{M} &= -\chi \frac{2A^2 M N_2}{P},\\
\dot{B}_2 &= -\alpha_1 \frac{10A^2 B_2^2}{P} + \alpha_3 \frac{PB_2}{A} + \alpha_1 \frac{6A^2 B_2 R_2}{P} + \alpha_1 \frac{12A^2 B_4}{P}\\
&\quad - \alpha_2 \frac{4AM^2 N_2^2}{P} - \alpha_3 \frac{PR_2}{A},\\
\dot{R}_2 &= -\beta_1 \frac{12A^2 B_2 R_2}{P} + \beta_1 \frac{8A^2 R_2^2}{P} - \beta_3 \frac{PR_2}{A} + \beta_1 \frac{12A^2 R_4}{P}\\
&\quad - \beta_2 \frac{4AM^2 N_2^2}{P} + \beta_3 \frac{PB_2}{A},\\
\dot{N}_2 &= -\chi \frac{12A^2 B_2 N_2}{P} + \chi \frac{2A^2 N_2^2}{P} + \chi \frac{6A^2 N_2 R_2}{P} + \chi \frac{12A^2 N_4}{P},\\
\dot{B}_4 &= -\alpha_1 \frac{58A^2 B_2 B_4}{P} + \alpha_3 \frac{PB_4}{A} + \alpha_1 \frac{10A^2 B_2^3}{P} - \alpha_1 \frac{20A^2 B_2^2 R_2}{P}\\
&\quad + \alpha_1 \frac{10A^2 B_2 R_2^2}{P} + \alpha_1 \frac{10A^2 B_2 R_4}{P} + \alpha_1 \frac{20A^2 B_4 R_2}{P} + \alpha_1 \frac{30A^2 B_6}{P}\\
&\quad + \alpha_2 \frac{8AB_2 M^2 N_2^2}{P} - \alpha_2 \frac{4AM^2 N_2^2 R_2}{P} - \alpha_2 \frac{16AM^2 N_2 N_4}{P} - \alpha_3 \frac{PR_4}{A},\\
\dot{R}_4 &= -\beta_1 \frac{40A^2 B_2 R_4}{P} + \beta_1 \frac{2A^2 R_2 R_4}{P} - \beta_3 \frac{PR_4}{A} + \beta_1 \frac{10A^2 B_2^2 R_2}{P}\\
&\quad - \beta_1 \frac{20A^2 B_2 R_2^2}{P} - \beta_1 \frac{20A^2 B_4 R_2}{P} + \beta_1 \frac{10A^2 R_2^3}{P} + \beta_1 \frac{30A^2 R_2 R_4}{P}\\
&\quad + \beta_1 \frac{30A^2 R_6}{P} + \beta_2 \frac{4AB_2 M^2 N_2^2}{P} - \beta_2 \frac{16AM^2 N_2 N_4}{P} + \beta_3 \frac{PB_2^2}{A}\\
&\quad - \beta_3 \frac{2B_2 PR_2}{A} + \beta_3 \frac{B_4 P}{A} + \beta_3 \frac{PR_2^2}{A},\\
\dot{N}_4 &= -\chi \frac{40A^2 B_2 N_4}{P} + \chi \frac{2A^2 N_2 N_4}{P} + \chi \frac{10A^2 B_2^2 N_2}{P} - \chi \frac{20A^2 B_2 N_2 R_2}{P}\\
&\quad - \chi \frac{20A^2 B_4 N_2}{P} + \chi \frac{10A^2 N_2 R_2^2}{P} + \chi \frac{10A^2 N_2 R_4}{P} + \chi \frac{20A^2 N_4 R_2}{P}\\
&\quad + \chi \frac{30A^2 N_6}{P},\\
&\ldots.
\end{aligned}
\tag{30}
$$

An immediate idea of how to solve (30) could be to truncate the system by removing higher-order variables and solve the resulting closed system under some initial conditions. However, such an approach has a serious flaw since there is no guarantee that the three fronts—the energy front, dissipation front, and velocity front—would coincide during the evolution. By the physics of diffusion, if the fronts do not coincide initially, they must catch up with each other. Suppose, for example, that initially the velocity front is behind the energy and dissipation fronts (suppose that these two coincide). Then the turbulent diffusion will instantaneously transfer the momentum forward up to the energy/dissipation front position. Conversely, if the velocity front

is initially ahead of the energy/dissipation front, it will be motionless for some time, as there is no turbulence in its vicinity. The velocity front would move only when the energy/dissipation front catches up, after which all the fronts move together. The front $x = h(t)$, where the energy, dissipation, and velocity decrease to a zero level, is a special point, yet the system (30) "does not know about it." We should explicitly impose the physical condition that the three profiles (29) must meet at the point $(K = \varepsilon = u = 0,\ x = h)$.

Let us demonstrate with a simple example that the lack of such a condition leads to the growth of the gap between the fronts. Consider a relatively simple model

$$\partial_t K = \partial_x(K\partial_x K),$$
$$\partial_t u = \partial_x(K\partial_x u),$$

without attributing any physical sense to K and u. We look for power-series solutions in the form of (29) and transfer to the new time by using $AB_2\,dt = d\tau$. Retaining only two leading equations for the series coefficients and removing terms with B_4 and N_4, we have

$$\begin{aligned} B_2' &= -4B_2, \\ N_2' &= -6N_2 + \frac{2N_2^2}{B_2}. \end{aligned} \tag{31}$$

Upon solving (31), the front of K can be determined from

$$1 - B_2 h_K^2 = 0,$$

and the front of u can be found from

$$1 - N_2 h_u^2 = 0.$$

Clearly $N_2 = B_2$ satisfies (31), but is this solution stable? Introduce the perturbation s by

$$N_2 = B_2 - s. \tag{32}$$

Substituting (32) into (31) and linearizing, we get

$$s' = -2s.$$

The perturbation decays as $\exp(-2\tau)$, whereas B_2 decays, according to (31), as $\exp(-4\tau)$. Thus, the perturbation goes to zero slower than the function itself. This leads to a large discrepancy between the values of B_2 and N_2, and hence in the front positions, $h_u^2 = 1/N_2$ and $h_K^2 = 1/B_2$. A similar effect occurs with the system (30).

Let us see how the situation changes if we require that the fronts coincide. We augment (31) by two extra equations stating that the functions turn into zero at the same point $x = h(t)$, that is, $K(h,t) = 0$ and $u(h,t) = 0$, where K and u are represented by the truncated series (29). The two extra equations bring one extra unknown, h. Therefore we need to add another unknown to have as many equations as unknowns. Let this new unknown be N_4. We get

$$\begin{aligned} B_2' &= -4B_2, \\ N_2' &= -6N_2 + \frac{12N_4}{B_2} + \frac{2N_2^2}{B_2}, \\ 1 - B_2 h^2 &= 0, \\ 1 - N_2 h^2 - N_4 h^4 &= 0. \end{aligned} \tag{33}$$

Excluding h and N_4 from (33) leads to

$$
\begin{aligned}
B_2' &= -4B_2,\\
N_2' &= -6N_2 + \frac{2N_2^2}{B_2} + 12(B_2 - N_2).
\end{aligned}
\tag{34}
$$

Substituting (32) into (34) and linearizing gives

$$s' = -14s.$$

Now s decays much faster than B_2 so that, in contrast to the previous case, B_2 and N_2 become closer to each other.

Applying a similar approach to the system (30), we require that K, ε, and u turn into zero at the same location $x = h(t)$. Retaining in the power-series (29) only terms up to the fourth order, we require

$$
\begin{aligned}
1 - B_2h^2 - B_4h^4 &= 0,\\
1 - R_2h^2 - R_4h^4 &= 0,\\
1 - N_2h^2 - N_4h^4 &= 0.
\end{aligned}
\tag{35}
$$

Equations (35) are complemented by the truncated dynamic equations (30),

$$
\begin{aligned}
\dot{A} &= -\alpha_1\frac{2A^3B_2}{P} - \alpha_3 P,\\
\dot{P} &= -\beta_1 2A^2R_2 - \beta_3\frac{P^2}{A},\\
\dot{M} &= -\chi\frac{2A^2MN_2}{P},\\
\dot{B}_2 &= -\alpha_1\frac{10A^2B_2^2}{P} + \alpha_3\frac{PB_2}{A} + \alpha_1\frac{6A^2B_2R_2}{P} + \alpha_1\frac{12A^2B_4}{P}\\
&\quad - \alpha_2\frac{4AM^2N_2^2}{P} - \alpha_3\frac{PR_2}{A},\\
\dot{R}_2 &= \beta_1\frac{8A^2R_2^2}{P} - \beta_3\frac{PR_2}{A} - \beta_1\frac{12A^2B_2R_2}{P} + \beta_1\frac{12A^2R_4}{P}\\
&\quad - \beta_2\frac{4AM^2N_2^2}{P} + \beta_3\frac{PB_2}{A},\\
\dot{N}_2 &= \chi\frac{2A^2N_2^2}{P} - \chi\frac{12A^2B_2N_2}{P} + \chi\frac{6A^2N_2R_2}{P} + \chi\frac{12A^2N_4}{P},\\
\dot{B}_4 &= -\alpha_1\frac{58A^2B_2B_4}{P} + \alpha_3\frac{PB_4}{A} + \alpha_1\frac{10A^2B_2^3}{P} - \alpha_1\frac{20A^2B_2^2R_2}{P}\\
&\quad + \alpha_1\frac{10A^2B_2R_2^2}{P} + \alpha_1\frac{10A^2B_2R_4}{P} + \alpha_1\frac{20A^2B_4R_2}{P} + \alpha_1\frac{30A^2B_6}{P}\\
&\quad + \alpha_2\frac{8AB_2M^2N_2^2}{P} - \alpha_2\frac{4AM^2N_2^2R_2}{P} - \alpha_2\frac{16AM^2N_2N_4}{P} - \alpha_3\frac{PR_4}{A}.
\end{aligned}
\tag{36}
$$

The system (35)–(36) contains 10 equations with respect to 10 time-dependent functions: A, P, M, B_2, R_2, N_2, B_4, R_4, N_4, and h.

As before, we "create" linear terms by modifying time:

$$\frac{d}{(A^2B_2/P)\,dt} = \frac{d}{d\tau} \equiv ()'. \tag{37}$$

Dividing (36) by A^2B_2/P and converting to τ results in

$$\begin{aligned}
A' &= -\alpha_1 2A - \alpha_3 \frac{P^2}{A^2B_2},\\
P' &= -\beta_1 \frac{2R_2P}{B_2} - \beta_3 \frac{P^3}{A^3B_2},\\
M' &= -\chi \frac{2MN_2}{B_2},\\
B_2' &= -\alpha_1 10B_2 + \alpha_3 \frac{P^2}{A^3} + \alpha_1 6R_2 + \alpha_1 \frac{12B_4}{B_2}\\
&\quad - \alpha_2 \frac{4M^2N_2^2}{AB_2} - \alpha_3 \frac{P^2R_2}{A^3B_2},\\
R_2' &= -\beta_1 12R_2 + \beta_1 \frac{8R_2^2}{B_2} - \beta_3 \frac{P^2R_2}{A^3B_2} + \beta_1 \frac{12R_4}{B_2}\\
&\quad - \beta_2 \frac{4M^2N_2^2}{AB_2} + \beta_3 \frac{P^2}{A^3},\\
N_2' &= -\chi 12N_2 + \chi \frac{2N_2^2}{B_2} + \chi \frac{6N_2R_2}{B_2} + \chi \frac{12N_4}{B_2},\\
B_4' &= -\alpha_1 58B_4 + \alpha_3 \frac{P^2B_4}{A^3B_2} + \alpha_1 10B_2^2 - \alpha_1 20B_2R_2\\
&\quad + \alpha_1 10R_2^2 + \alpha_1 10R_4 + \alpha_1 \frac{20B_4R_2}{B_2} + \alpha_1 \frac{30B_6}{B_2}\\
&\quad + \alpha_2 \frac{8M^2N_2^2}{A} - \alpha_2 \frac{4M^2N_2^2R_2}{AB_2} - \alpha_2 \frac{16M^2N_2N_4}{AB_2} - \alpha_3 \frac{P^2R_4}{A^3B_2}.
\end{aligned} \tag{38}$$

Figures 3, 4, and 5 display some trajectories for the system (35)–(38). We used $\alpha_1 = 0.09$, $\alpha_2 = 0.09$, $\alpha_3 = 1$, $\beta_1 = 0.07$, $\beta_2 = 0.13$, $\beta_3 = 1.92$, $\chi = 0.09$. The initial conditions were chosen to ensure the same position for the three fronts.

Figure 6 shows the front propagation. Note that the seeming acceleration occurs only in terms of the artificial time τ. In terms of the real time t the graph will have opposite curvature showing deceleration.

We notice a considerable spectral gap between the linear decay rates in (36): the coefficient at B_4, $(-58\alpha_1)$, is from 5 to 6 times larger than that of B_2, $(-10\alpha_1)$, of R_2, $(-12\beta_1)$, and of N_2, (-12χ). The numerical data show that the linear terms are the largest in absolute value in each dynamic equation.

The numerical data also show that on the initial sections of the trajectories the velocity terms M, N_2, and N_4 in the equation $B_4' = \ldots$ are much smaller than the terms associated with the energy and dissipation. However, after some period of time the velocity-associated terms become comparable to the other terms.

This points to a mechanism characteristic of center manifolds, where some variables, such as B_4 in our problem, rapidly decay until they are small enough to be comparable with the nonlinear terms which come into play.

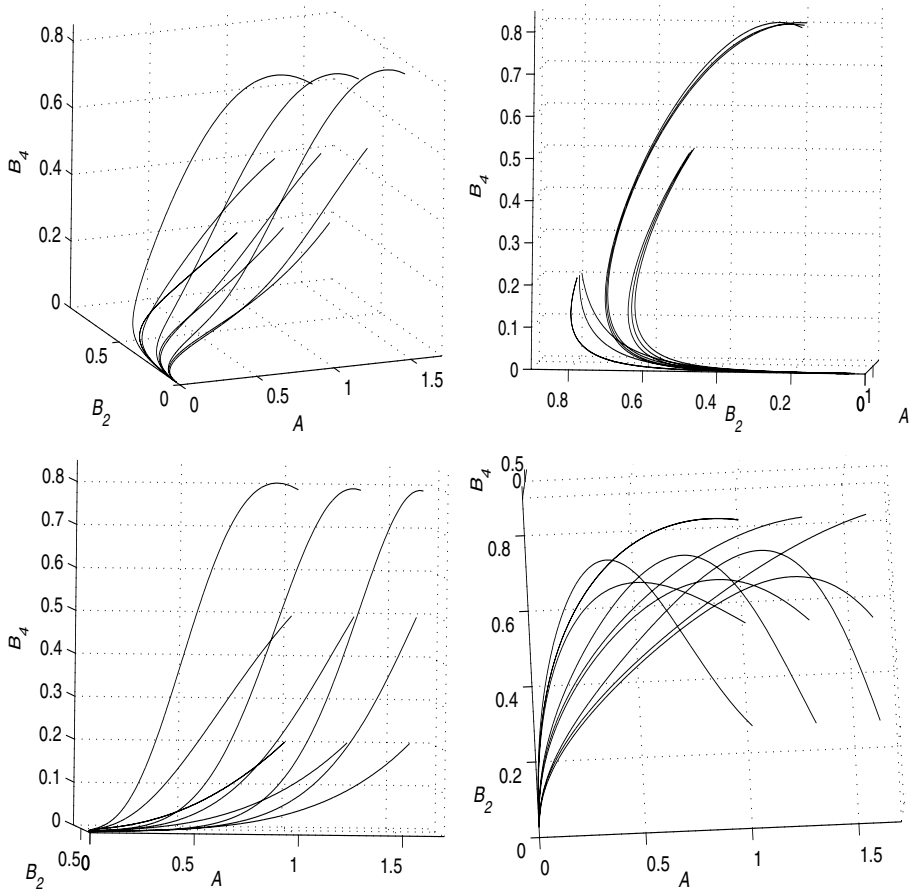

FIG. 3. *Trajectories for the model* (35)–(38) *in the space of the energy variables.*

To illustrate this mechanism we use a simple example from [20]:

$$\begin{aligned} \dot{x} &= -px - xy, \\ \dot{y} &= -y + x^2 - 2y^2. \end{aligned} \tag{39}$$

The linear decay rate p of x is much smaller than that of y, say $p = 0.1 \ll 1$. A set of trajectories for the system (39) is shown in Figure 7. See that the trajectories are attracted to a single curve. It can be shown that in the limit $p = 0$ the attractor is exactly

$$y = x^2, \tag{40}$$

which is called the center manifold. Driven by the linear term $(-y)$ the trajectories quickly drop onto the manifold on which the nonlinear terms $(x^2 - 2y^2)$ are comparable to $(-y)$. On the attractor, in view of (40), the motion is described by $\dot{x} = -xy = -x^3$. The variable y depends on t through x to which it is rigidly linked by (40).

We anticipate that a similar situation takes place in our problem with B_4 being analogous to y in the above example. However, the problem is complicated by a multitude of variables. In this paper we investigate a simplified version of the model.

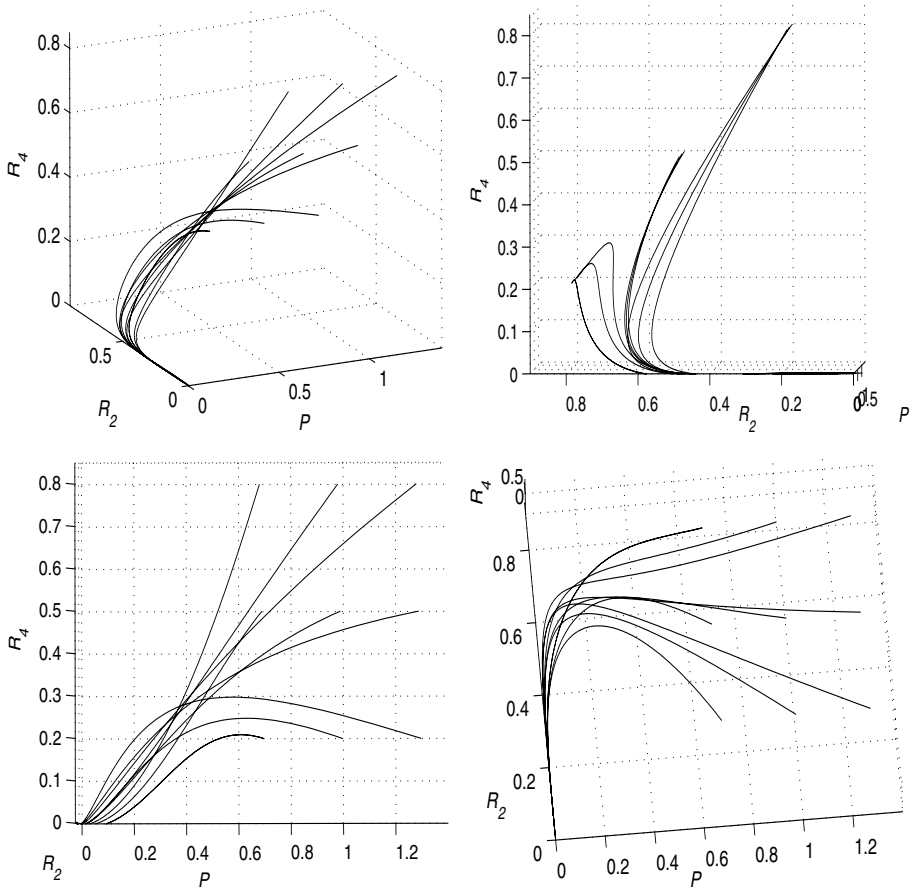

FIG. 4. *Trajectories for the model* (35)–(38) *in the space of the dissipation variables.*

4. Reduced version of the model. In this section we simplify the K-ε model (28) to a great extent, yet make sure that the key physical factors remain. These factors are the nonlinear diffusion and the coupling via the velocity shear. We will keep calling K the energy and u the velocity for consistency with the previous section. However, these terms should not be directly associated with the physical quantities. If we find attractors, our approach will provide a useful basis for studies of more complicated systems.

We assume that (a) $\alpha_3 = \beta_3 = 0$ to remove the dissipation terms, (b) $\alpha_1 = \alpha_2 = \beta_1 = \beta_2 = 1$ for simplicity, and (c) initial conditions for K and ε coincide. Thus, the problem formulations for K and ε become identical; therefore $K \equiv \varepsilon$ at all times, that is, $A(t) \equiv P(t)$ and $B_k(t) \equiv R_k(t)$, $k = 2, 4, \ldots$. As a result, system (28) reduces to the two equations

$$\begin{aligned} \partial_t K &= \partial_x \left(K \partial_x K \right) + K \left(\partial_x u \right)^2 , \\ \partial_t u &= \partial_x \left(K \partial_x u \right) . \end{aligned} \tag{41}$$

The manipulations in section 3 automatically apply to (41). The definition of new time (37) transforms into

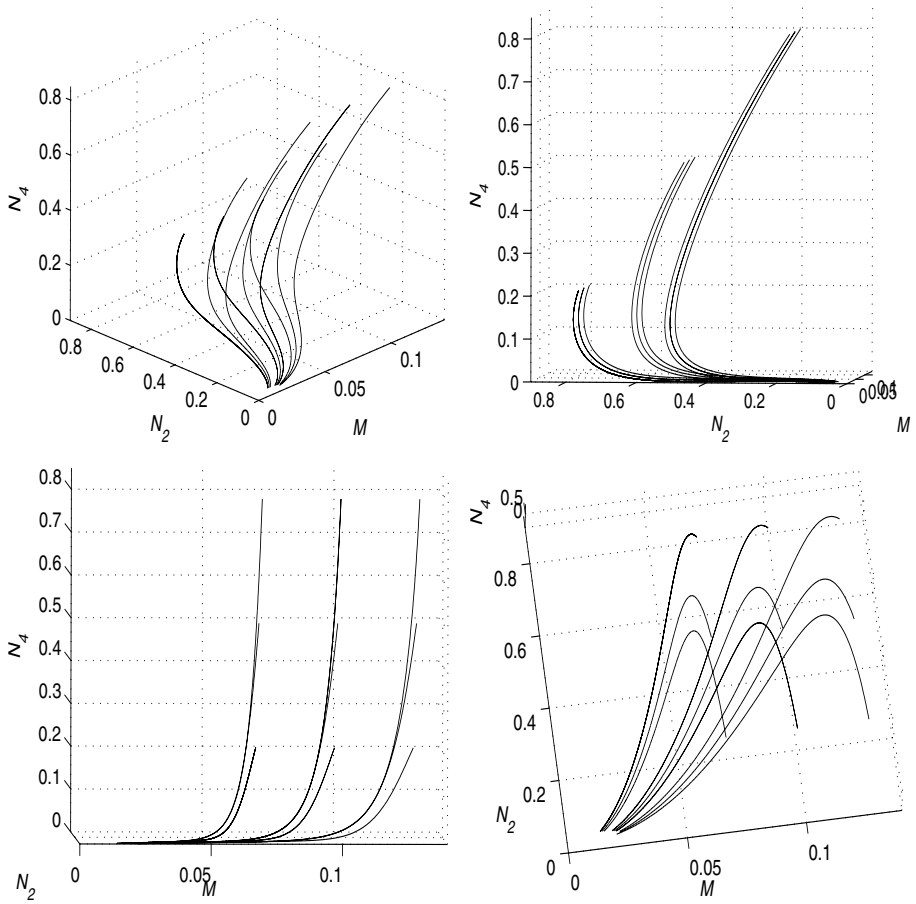

FIG. 5. *Trajectories for the model* (35)–(38) *in the space of the velocity variables.*

$$\frac{d}{(AB_2)\,dt} = \frac{d}{d\tau} \equiv ()'. \tag{42}$$

We introduce the new function

$$T \equiv \frac{M^2}{A}. \tag{43}$$

It turns out that it is possible to derive a dynamic equation for T, where M and A appear in combination (43). This equation will replace the two dynamic equations for A and M. Differentiating (43) gives

$$T' = \left(\frac{M^2}{A}\right)' = \frac{2MM'A - M^2A'}{A^2}. \tag{44}$$

The following expressions for A' and M' are obtained from (38) under conditions (a), (b), and (c): $A' = -2A$ and $M' = -2MN_2/B_2$. Substituting these into (44) gives the equation shown below.

Under assumptions (a), (b), and (c), and in view of (44), system (35)–(38) becomes

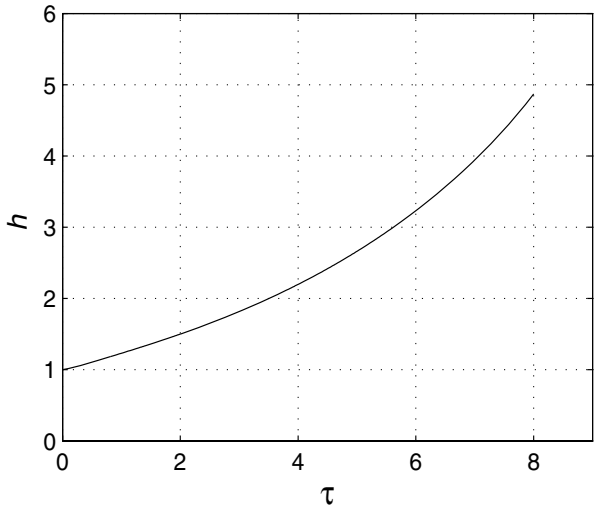

FIG. 6. *Propagation of the turbulent front in the model* (35)–(38).

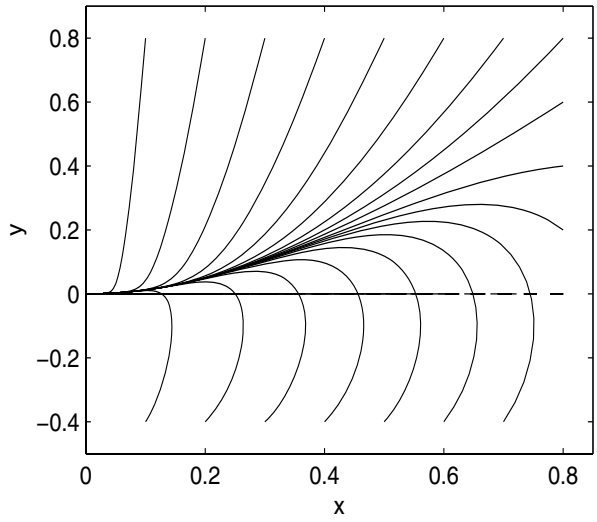

FIG. 7. *Center manifold in model* (39).

$$
\begin{aligned}
&T' = -\frac{4N_2T}{B_2} + 2T,\\
&B_2' = -4B_2 - \frac{4N_2^2T}{B_2} + \frac{12B_4}{B_2},\\
&N_2' = -6N_2 + \frac{2N_2^2}{B_2} + \frac{12N_4}{B_2},\\
&B_4' = -28B_4 + 4N_2^2T - \frac{16N_2N_4T}{B_2},\\
&1 - B_2h^2 - B_4h^4 = 0,\\
&1 - N_2h^2 - N_4h^4 = 0.
\end{aligned}
\tag{45}
$$

System (45) contains six equations with respect to six unknown functions: T, B_2, N_2, B_4, N_4, and h. We solved (45) numerically, making sure that the initial positions of the energy and velocity fronts coincide.

Using the data from the numerical experiments we can deduce results in analytical form. According to the data, at large times some terms in (45) become negligible, namely, $(-16N_2N_4T/B_2)$ in the equation $B_4' = \ldots$, $(12B_4/B_2)$ and $(-4N_2^2T/B_2)$ in the equation $B_2' = \ldots$, and $(12N_4/B_2)$ in the equation $N_2' = \ldots$. Also it is important to note $N_2 \to B_2$. Therefore from (45) we get *asymptotically*

$$T' = -2T, \quad N_2' = -4N_2, \quad B_2 = N_2, \tag{46}$$

from which we get

$$T = T_0 e^{-2(\tau-\tau_0)}, \quad B_2 = N_2 = N_0 e^{-4(\tau-\tau_0)}, \tag{47}$$

where τ_0, T_0, and N_0 are some reference values. Substituting (47) into (45), we get

$$B_4' = -28B_4 + 4N_0^2 T_0 e^{-10(\tau-\tau_0)}. \tag{48}$$

The solution of the homogeneous part of (48), $\sim \exp[-28(\tau-\tau_0)]$, expresses the decay caused by the linear term $(-28B_4)$. This part of the solution is negligible compared to the solution of the nonhomogeneous equation,

$$B_4 = Ce^{-10(\tau-\tau_0)}, \tag{49}$$

expressing the forced dynamics of B_4.

Here we recognize the center manifold mechanism: a rapid decay of a function to a level where the linear term becomes comparable to the nonlinear term. It is easy to find the constant by substituting (49) into (48),

$$C = \frac{2}{9}N_0^2 T_0.$$

Hence, the variable B_4 is attracted to the manifold described by

$$B_4(\tau) = \frac{2}{9}N_0^2 T_0 \exp[-10(\tau-\tau_0)] = \frac{2}{9}N_2^2 T$$

or, using (43),

$$B_4 = \frac{2N_2^2 M^2}{9A}. \tag{50}$$

Let us use the numerical data directly to show that B_4 is indeed attracted to (50). There are many ways to demonstrate the attraction, and below we implement just one of them. A graph B_4 versus N_2^2 and T would be a curved surface. We go over to new variables, in terms of which the surface would be a plane,

$$N_2^2 = \xi + \eta, \quad T = \xi - \eta. \tag{51}$$

The product $N_2^2 T$ is represented by a plane in terms of ξ^2 and η^2:

$$N_2^2 T = \xi^2 - \eta^2. \tag{52}$$

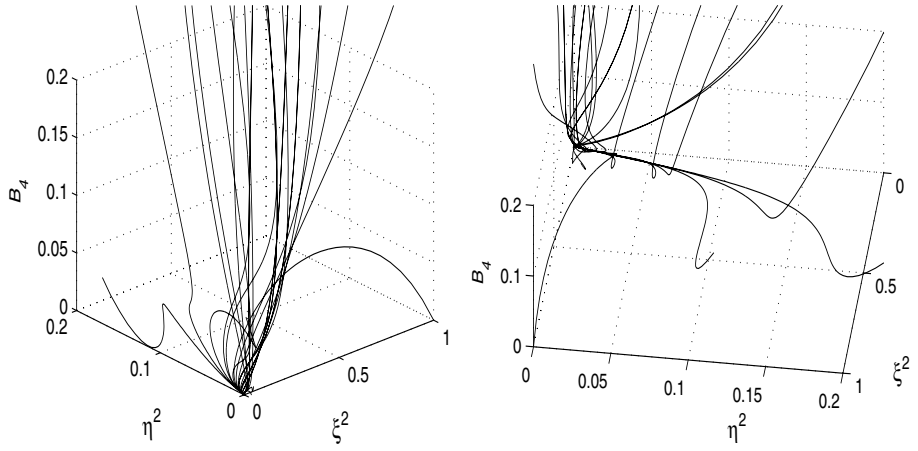

FIG. 8. *Trajectories for the reduced model* (45).

The new variables are defined by (51),

$$\xi = \frac{1}{2}\left(N_2^2 + T\right), \quad \eta = \frac{1}{2}\left(N_2^2 - T\right).$$

Figure 8 gives two views of a set of trajectories in the space (ξ^2, η^2). The right-hand view shows that all the trajectories converge to a surface which, from this particular angle, appears as a straight line. Clearly the surface is a plane.

In order to obtain a closed system from (35)–(38), we removed the term with B_6 from the equation $B_4' = \ldots$ and obtained the dynamics of N_4 from the front equation $1 - N_2h^2 - N_4h^4 = 0$ rather than from the respective dynamic equation.

To let N_4 evolve according to the dynamic law, we add the equation $N_4' = \ldots$. Adding the extra equation makes it necessary to add another unknown to the system, say B_6 (or alternatively, N_6; however, this is not of principle importance):

$$\begin{aligned}
T' &= -\frac{4N_2T}{B_2} + 2T,\\
B_2' &= -4B_2 - \frac{4N_2^2T}{B_2} + \frac{12B_4}{B_2},\\
N_2' &= -6N_2 + \frac{2N_2^2}{B_2} + \frac{12N_4}{B_2},\\
B_4' &= -28B_4 + 4N_2^2T - \frac{16N_2N_4T}{B_2} + \frac{30B_6}{B_2},\\
N_4' &= -20N_4 + \frac{2N_2N_4}{B_2} - \frac{10N_2B_4}{B_2},\\
1 &- B_2h^2 - B_4h^4 - B_6h^6 = 0,\\
1 &- N_2h^2 - N_4h^4 = 0.
\end{aligned} \tag{53}$$

Trajectories for the system (53) are shown in Figure 9. We see the same attractor as for the shorter version (45). In the dynamic equation $B_4' = \ldots$ the new term $(30B_6/B_2)$ and the old term $(-16N_2N_4T/B_2)$ are smaller than the other terms by two orders of magnitude.

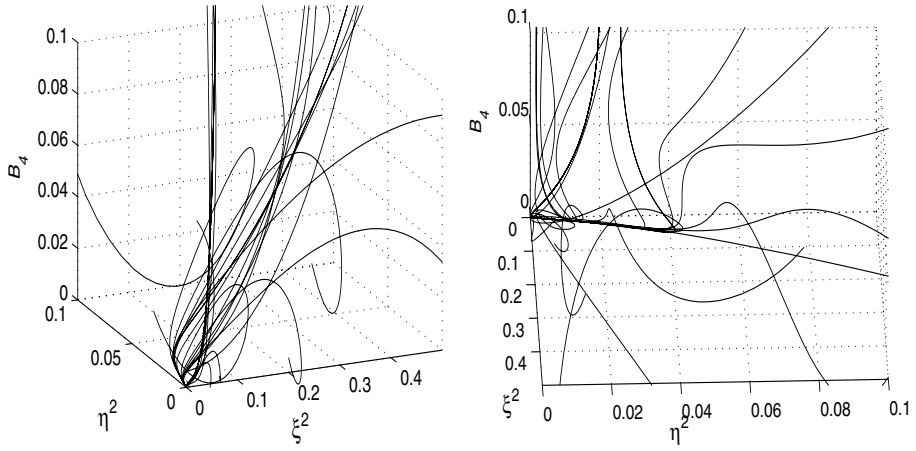

FIG. 9. *Trajectories for the enhanced version* (53) *of the reduced model.*

Now we look for an attractor for N_4. Substituting $N_2 = B_2$ (we emphasize that this relation is asymptotic, not exact) and the expression for B_4, (50), into the equation $N_4' = \dots$ in (53) we get

$$N_4' = -18N_4 - \frac{20}{9}N_0^2 T_0 e^{-10(\tau-\tau_0)}. \tag{54}$$

As in the case for B_4, the solution of the homogeneous part of this equation rapidly decays as $\exp[-18(\tau - \tau_0)]$ so that the solution is virtually the forced one,

$$N_4 = De^{-10(\tau-\tau_0)}. \tag{55}$$

Substituting (55) into (54) gives $D = -5N_0^2 T_0/18$, and therefore the attractor is

$$N_4 = -\frac{5N_2^2 M^2}{18A}. \tag{56}$$

A graph N_4 against ξ^2 and η^2 is again a plane, as is evident from Figure 10.

Remarkably, dividing (50) by (56), we find

$$\frac{B_4}{N_4} = -\frac{4}{5} \tag{57}$$

on the attractor. The dependence B_4/N_4 versus time in the numerical experiments is given in Figure 11. It clearly shows the attraction to the predicted value $(-4/5) = -0.8$.

Further extension of the model can be done by involving the equation $B_6' = \dots$ (without the term with B_8). Accordingly we need to add another unknown, for instance, N_6, to make the front equation $1 - N_2h^2 - N_4h^4 - N_6h^6 = 0$. This process can be continued.

More equations would give a more accurate description; however, the result about the existence of the attractors (50) and (56) holds.

In summary, the solutions of the confined-source problem for the quasi–fluid-dynamical system $\partial_t K = \partial_x (K\partial_x K) + K(\partial_x u)^2$, $\partial_t u = \partial_x (K\partial_x u)$ converge to the

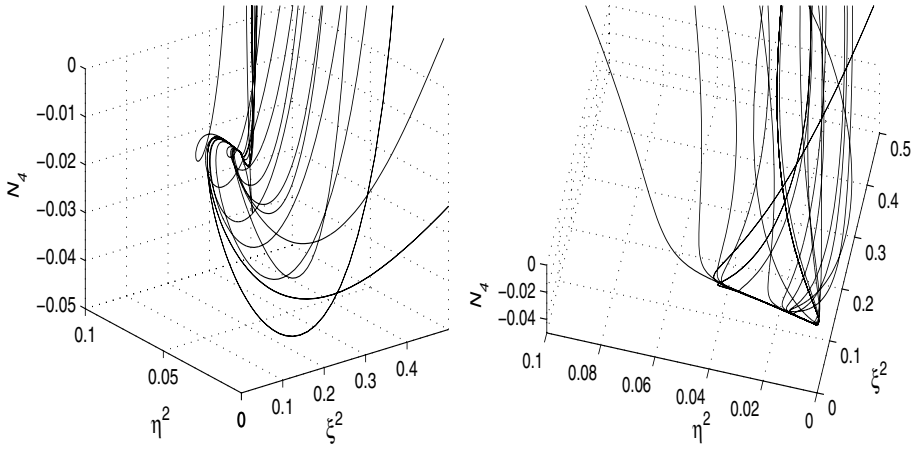

FIG. 10. *Trajectories for the enhanced version* (53) *of the reduced model.*

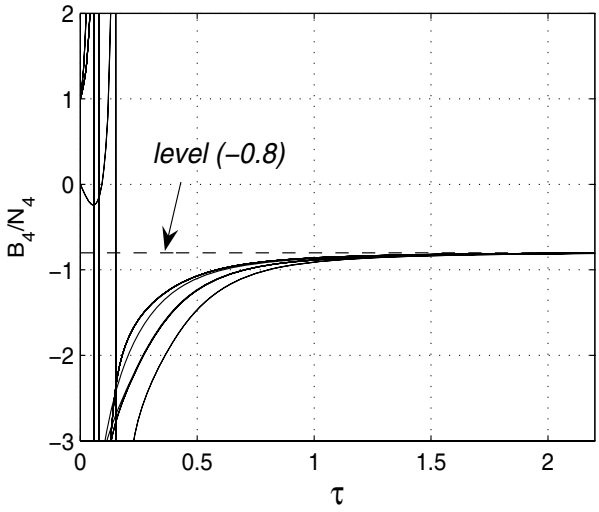

FIG. 11. *The ratio B_4/N_4 versus time.*

attractor

$$K = A\,(1 - B_2x^2 - B_4x^4 - \cdots),$$
$$u = M\,(1 - N_2x^2 - N_4x^4 - \cdots),$$

where

$$B_4 = \frac{2N_2^2M^2}{9A}, \quad N_4 = -\frac{5N_2^2M^2}{18A} \tag{58}$$

and the variables A, M, B_2, and N_2 evolve according to (43), (53). (Note that one should not substitute the asymptotic result (58) into (53) and then solve for A, M, B_2, and N_2. This would break stability, similarly to example (34). If in (34) one replaces $12(B_2 - N_2)$ by its asymptotic value zero, the system becomes unstable; see (31).)

5. Conclusions. We considered a process of an expansion of a turbulent jet driven by turbulent diffusion. The mathematical model essentially involves coupling between the turbulent energy, dissipation, and momentum. Looking for solutions in the form of power-series in a spatial coordinate, we derived dynamical systems with respect to time-dependent series coefficients. The system is essentially nonlinear; however, modifying time allowed us to create linear terms, which dominate during the early dynamics. We analyzed in detail a simplified version of the model with a radically reduced number of variables. The numerical and analytical analyses allowed us to find an attractor in exact form.

REFERENCES

[1] M. Muskat, *The Flow of Homogeneous Fluids through Porous Media*, McGraw-Hill, New York, 1937.
[2] D. G. Aronson, *The porous medium equation*, in Nonlinear Diffusion Problems, Lecture Notes in Math. 1224, A. Fasano and M. Primicerio, eds., Springer, Berlin, 1986, pp. 1–46.
[3] J. Buckmaster, *Viscous sheets advancing over dry beds*, J. Fluid Mech., 81 (1977), pp. 735–756.
[4] J. R. King, *The isolation oxidation of silicon: The reaction-controlled case*, SIAM J. Appl. Math., 49 (1989), pp. 1064–1080.
[5] J. L. Vazquez, *Hyperbolic aspects in the theory of the porous media equation*, in Metastability and Incompletely Posed Problems, S. Antman et al., eds., Springer, New York, 1987, pp. 325–342.
[6] L. A. Peletier, *The porous media equation*, in Applications of Nonlinear Analysis in the Physical Sciences, H. Amann et al., eds., Pitman, London, 1981, pp. 229–241.
[7] D. G. Aronson, *Nonlinear diffusion problems*, in Free Boundary Problems: Theory and Applications I, Res. Notes in Math. 78, A. Fasano and M. Primicerio, eds., Pitman, London, 1983, pp. 135–149.
[8] F. Bernis, *Viscous flows, fourth order nonlinear degenerate parabolic equations and singular elliptic problems*, in Free Boundary Problems: Theory and Applications, Pitman Res. Notes Math. Ser. 323, J. I. Diaz, M. A. Herrero, A. Linan, and J. L. Vazquez, eds., Longman Sci. Tech., Harlow, 1995, pp. 40–56.
[9] J. W. Barrett, J. F. Blowey, and H. Garcke, *Finite element approximation of a fourth order nonlinear degenerate parabolic equation*, Numer. Math., 80 (1998), pp. 525–556.
[10] J. D. Evans, M. Vynnycky, and S. P. Ferro, *Oxidation-induced stresses in the isolation oxidation of silicon*, J. Engrg. Math., 38 (2000), pp. 191–218.
[11] J. W. Barrett, S. Langdon, and R. Nurnberg, *Finite element approximation of sixth order nonlinear degenerate parabolic equation*, Numer. Math., 96 (2004), pp. 401–434.
[12] Ya. B. Zel'dovich and A. S. Kompaneets, *On the theory of heat propagation for temperature dependent thermal conductivity*, in Collection Commemorating the 70th Anniversary of A. F. Joffe, Izv. Akad. Nauk SSSR, 1950, pp. 61–71.
[13] A. D. Polyanin and V. F. Zaitsev, *Handbook of Nonlinear Partial Differential Equations*, Chapman and Hall/CRC, Boca Raton, FL, 2004.
[14] N. F. Smyth and J. M. Hill, *High-order nonlinear diffusion*, IMA J. Appl. Math., 40 (1988), pp. 73–86.
[15] D. V. Strunin and A. J. Roberts, *Self-similarity of decaying turbulent layer*, in Proceedings of the 5th Biennial Engineering Mathematics and Applications Conference (EMAC-2002), The Institution of Engineers, Brisbane, Australia, pp. 205–210.
[16] C. G. Speziale, *Analytical methods for the development of Reynolds-stress closures in turbulence*, in Annual Review of Fluid Mechanics, Vol. 23, Annual Reviews, Palo Alto, CA, 1991, pp. 107–157.
[17] B. E. Launder, G. J. Reece, and W. Rodi, *Progress in the development of a Reynolds-stress turbulence closure*, J. Fluid Mech., 68 (1975), pp. 537–566.
[18] K. Hanjalic and B. E. Launder, *A Reynolds stress model of turbulence and its applications to thin shear flows*, J. Fluid Mech., 52 (1972), pp. 609–638.
[19] A. J. Roberts, *Tony Roberts' Home Page Links to Information*, Department of Mathematics and Computing, University of Southern Queensland, Toowoomba, Australia, http://www.sci.usq.edu.au/staff/robertsa/ (2005).
[20] A. J. Roberts, *Appropriate initial conditions for asymptotic descriptions of the long term evolution of dynamical systems*, J. Austral. Math. Soc. Ser. B, 31 (1989), pp. 48–75.